

Radiation-Pressure-Induced Hierarchical Structure of Liquid-Crystalline Inorganic Nanosheets

Makoto Tominaga,[†] Takashi Nagashita,[‡] Takuya Kumamoto,[¶] Yuki Higashi,[§] Toshiaki Iwai,[‡] Teruyuki Nakato,^{*,¶} Yasutaka Suzuki,^{†,‡,§} Jun Kawamata^{*,†,‡,§}

[†]Graduate School of Medicine, Yamaguchi University, 1677-1 Yoshida, Yamaguchi-shi, Yamaguchi 753-8512, Japan

[‡]Graduate School of Sciences and Technology for Innovation, Yamaguchi University, 1677-1 Yoshida, Yamaguchi-shi, Yamaguchi 753-8512, Japan

[§]Faculty of Science, Department of Biology and Chemistry, Yamaguchi University, 1677-1 Yoshida, Yamaguchi-shi, Yamaguchi 753-8512, Japan

[¶]Department of Applied Chemistry, Kyusyu Institute of Technology, 1-1 Sensui-cho, Tabata-ku, Kitakyusyu-shi, Fukuoka 804-8550, Japan

[‡]Graduate School of Bio-Applications and System Engineering, Tokyo University of Agriculture and Technology, 2-24-16 Naka-cho, Koganei-shi, Tokyo 184-8588, Japan

ABSTRACT: Although hierarchical assemblies of colloidal particles add novel structure-based functions to systems, few local and on-demand colloidal structures have been developed. We have combined the colloidal liquid crystallinity of two-dimensional inorganic particles and laser radiation pressure to obtain a large hierarchical and local structure in a colloidal system. The scattering force of the laser beam converted the parallel nanosheet alignment to the direction of the incident laser beam. At the focal point, the nanosheet orientation depends on the electric field of the polarized laser beam. In contrast, a giant tree-ring-like nanosheet texture of more than 100 μm , and which is independent of the polarization direction, was organized at the periphery of the focal point. This organization resulted from a cooperative effect between the liquid-crystalline nanosheets, which indicates an effectiveness of optical manipulation to construct hierarchical colloidal structures with the aid of interparticle interactions.

KEYWORDS: colloid, inorganic nanosheet, liquid crystal, optical manipulation, radiation pressure

Hierarchical assemblies of particles that are formed by an external field application to colloidal particles are expected to serve as future functional materials. Electric and magnetic fields,^{1,2} shear,³ and laser-radiation pressures⁴⁻⁶ have been applied as external fields to manipulate colloidal nanoparticles. Laser radiation pressure achieves local and on-demand particle manipulation by optimizing irradiation conditions, such as the position of the focal point, the power, the polarization direction, and the shape of the wave-front of the incident laser beam. Particles such as polystyrene,⁷ glass beads,⁸ and biomolecules⁹ have been trapped at a focal point by the radiation pressure of a tightly focused laser beam. Microfabrication,¹⁰ selective optical transportation,¹¹ physical-

property measurements,¹² and the spectroscopic characterization¹³ of locally trapped particles have been conducted at a focal point.

In the last decade, the use of laser radiation pressure has been extended from simple optical manipulation or trapping to the organization of hierarchical structures. A laser beam that is focused on a nematic liquid crystal, 4'-pentyl-4-cyanobiphenyl yielded a new domain at around the focal point with a diameter of 24 μm , which was twenty times larger than that of the focal point.¹⁴ The formation of such a hierarchical structure was attributed to the re-orientation of liquid-crystalline molecules as determined by the balance between the generated optical and preexisting elastic torques of the nematic liquid crystal, based on the self-assembling ability, namely, the intermolecular interaction of the liquid crystal and the radiation pressure.

Hierarchical structures of colloidal particles have been constructed by using laser radiation pressure, although their formation is limited at interfaces. For example, colloidal polystyrene beads were assembled at an air-liquid interface to form a closely packed hierarchical structure with an assembly size of 20 μm , which was twenty times larger than that of the focal point.^{15,16} At an interface between the colloidal solution of the polystyrene beads and the glass substrate, beads assembled at the substrate surface to form a 30- μm -sized two-dimensional structure with horns; this size was thirty times larger than that of the focal point.¹⁷ These results suggest that laser irradiation of colloids evolves certain hierarchical structures that span from the focal point to the periphery at interfaces. However, reports on hierarchical structures that are larger than those of the focal points in colloidal systems are limited to the above examples, which have not used interparticle interactions effectively.

We used liquid-crystalline inorganic nanosheets for the colloidal particles. The

inorganic nanosheets are ~1-nm-thick plate-like particles with lateral dimensions of up to several micrometers, which exhibit lyotropic liquid crystallinity.¹⁸ One of the authors has studied liquid-crystalline nanosheet colloids that were prepared by exfoliation of layered niobates because of the high shape anisotropy of the colloidal particles. Niobate nanosheets are aligned in a lamellar manner with a basal spacing of several tens of nanometers in the liquid-crystalline state.¹⁹ Liquid-crystalline domains grow through self-assembly by incubating a liquid-crystalline niobate nanosheet colloid at room temperature to reach a sub-millimeter size.²⁰ The nanosheets respond to an external field, such as a shear force²¹ and an electric field.²² Hierarchical macroscopic structures can be formed in the liquid-crystalline nanosheet colloids by combining domain growth and an external field.^{20,23} However, with these methods, a colloid sample is organized in the same manner in the entire sample. The local and on-demand orientation by optical manipulation should expand the flexibility and arbitrary structural control of the nanosheet liquid crystals.

In this study, we constructed a laser-radiation-pressure-induced giant hierarchical structure of liquid-crystalline nanosheets. We irradiated a liquid-crystalline sample by using a focused laser beam of several milliwatts. As a result, we confirmed the local and on-demand formation of a 100 μm -sized hierarchical structure of niobate nanosheets.

RESULTS AND DISCUSSION

A niobate nanosheet colloid was prepared by exfoliating a layered $\text{K}_4\text{Nb}_6\text{O}_{17}$ in water at 5 gL^{-1} . The average lateral size of the niobate nanosheets was $1.6 \mu\text{m}$. The sample was injected into a $100\text{-}\mu\text{m}$ -thick thin-layer glass cell. The cell was set on the stage of an inverted microscope. Figure 1 shows the experimental setup. Optical microscope observations of the sample were conducted by using a 20-mW laser irradiation.

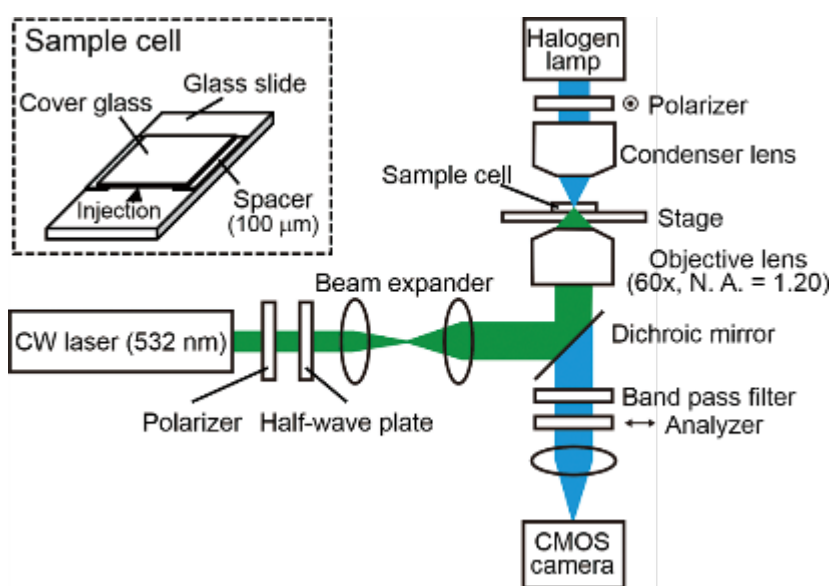


Figure 1. Experimental setup to observe the structural formation of niobate nanosheets with laser irradiation.

A video image under laser irradiation as observed with a polarized optical microscope is shown in the Supporting Information (Movie S1) and snapshots are provided in Figure 2. The image before laser irradiation was dark (Figure 2a), which indicates a homogeneous orientation of niobate nanosheets perpendicular to the propagation direction of the laser beam (hereafter, perpendicular orientation) in the thin-layer cell.²⁰ When the laser beam was irradiated, a birefringent spot appeared immediately at a focal point (Figure 2b). The appearance of birefringence indicates that niobate nanosheets were oriented parallel to the propagation direction of the laser beam (hereafter, parallel orientation).²⁰ After irradiating the laser beam for 15 s, a circularly textured additional birefringence area appeared at the periphery of the birefringence spot at the focal point (Figure 2c). Although the brightness of the additional area increased gradually until 120 s (Figures 2c–e), its 110- μm diameter, which was 370 times larger than that of the focal

point, was almost constant (see contrast-adjusted images in Supporting Information Figures S1). This result indicates that an orientational change of niobate nanosheets occurred at the periphery successive to that at the focal point under the laser irradiation.

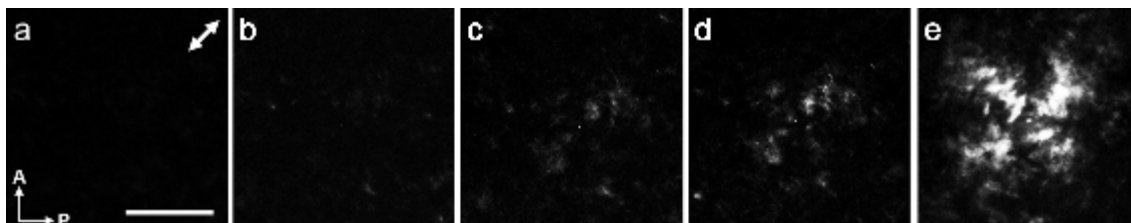


Figure 2. Polarized optical microscope images of a liquid-crystalline niobate nanosheet colloid (5 gL^{-1}) (a) before laser irradiation and (b) 2 s, (c) 15 s, (d) 40 s, and (e) 120 s after laser irradiation. The double arrow indicates the polarization direction of the incident laser beam. The scale bar denotes $50 \mu\text{m}$.

A parallel orientation that was induced by the laser irradiation was also observed by using a bright-field optical microscope. The video image is shown in the Supporting Information (Movie S2) and snapshots are given in Figure 3. The image before the laser irradiation was featureless (Figure 3a). This is consistent with the perpendicular orientation of nanosheets in the cell. After laser irradiation for 2 s, the image was the same as that before irradiation (Figure 3b). However, the magnified image, which is shown in Figure S2, demonstrates the presence of niobate nanosheets in a parallel orientation, which is the orientation along the polarization direction of the incident laser beam, at the focal point as evidenced by the appearance of line-shaped objects. The size of the domain of nanosheets in a parallel orientation increased gradually during laser irradiation. After laser-beam irradiation for 120 s, the domain diameter reached $15 \mu\text{m}$, which was 50 times larger than the focal-point diameter (Supporting Information, Figure S2). After laser-

beam irradiation for 40 s, another domain, which corresponds to the circularly textured additional birefringence area, appeared gradually at the periphery of the focal point (Figure 3d). In this domain, nanosheets in a parallel orientation formed a tree-ring texture with a diameter that increased to 80 μm after laser irradiation for 120 s (Figure 3e). This size was 270 times larger than the focal-point diameter.

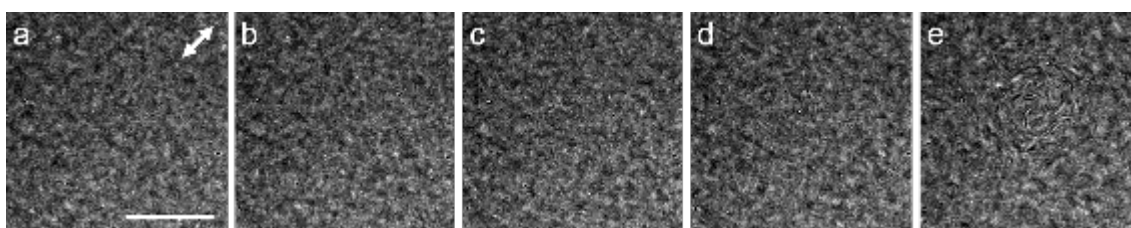


Figure 3. Bright-field optical microscope images of a liquid-crystalline niobate nanosheet colloid (5 gL^{-1}) (a) before laser irradiation and (b) at 2 s, (c) 15 s, (d) 40 s, and (e) 120 s after laser irradiation. The double arrow indicates the polarization direction of an incident laser beam. The scale bar denotes $50 \mu\text{m}$.

Figure 4 shows polarized optical microscope images of the liquid-crystalline niobate nanosheet colloid that was irradiated by rotating the polarization direction of the laser beam. The birefringent spot at the focal point was influenced significantly by the polarization direction of the laser beam. The spot was observed only when the polarization direction of the incident laser beam was nonparallel to the polarizer or analyzer of the microscope. However, the size and brightness of the circularly textured periphery of the focal point was unaffected by the polarization direction.

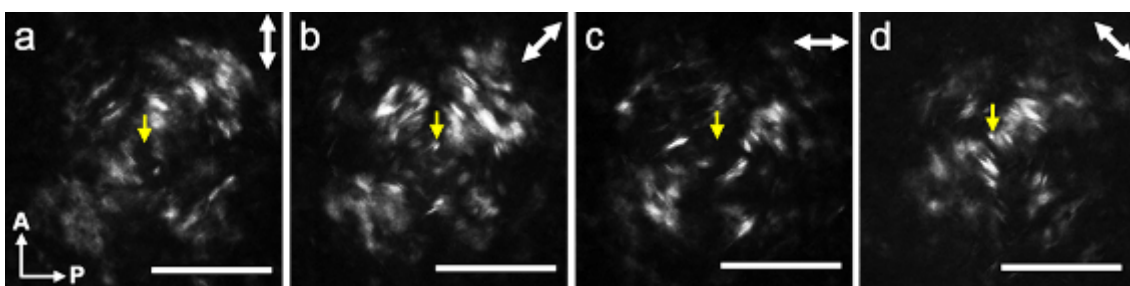


Figure 4. Polarized optical microscope images of a liquid-crystalline niobate nanosheet colloid (5 gL^{-1}) when the linear polarization of a laser beam was rotated. The double arrows indicate the polarization direction of an incident laser beam. The yellow arrows point to the position of the focal point. The scale bar denotes $50 \mu\text{m}$.

When the laser beam irradiated an isotropic niobate nanosheet colloid that was prepared at 0.05 gL^{-1} , niobate nanosheets were trapped only at the focal point; any structure larger than the focal point was not formed at the periphery. A movie of the isotropic colloid observed with a bright-field optical microscope with laser irradiation is shown in the Supporting Information (Movie S3) and snapshots are provided in Figure 5. Niobate nanosheets were dispersed randomly before the laser irradiation. After laser irradiation for 34 s, some nanosheets were assembled at the focal point. However, further nanosheet organization for the isotropic sample was not observed with the bright-field and polarized optical microscope (Supporting Information, Figure S3).

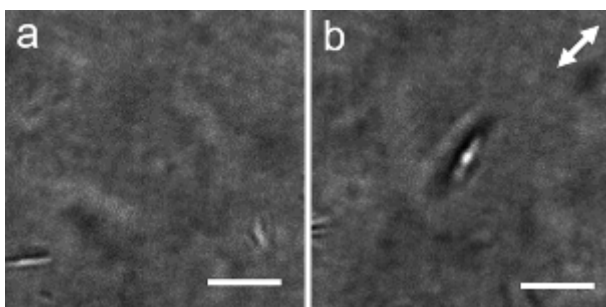


Figure 5. Bright-field optical microscope images of an isotropic niobate nanosheet

colloid (0.05 gL^{-1}) (a) before laser irradiation, (b) 34 s after laser irradiation. The double arrow indicates the polarization direction of an incident laser beam. The scale bar denotes $5 \mu\text{m}$.

As described above, when the laser beam irradiated a liquid-crystalline niobate nanosheet colloid, the nanosheet orientation changed from perpendicular to parallel with respect to the direction of laser beam. This orientational change is ascribed to a scattering force of the irradiated laser beam. The magnitude of the scattering force that is applied to an object is proportional to the number of photons that irradiate the object. The irradiated area where a nanosheet exists in a perpendicular orientation ($1.6 \mu\text{m} \times 1.6 \mu\text{m}$) is 1000 times larger than that where a nanosheet exists in a parallel orientation ($1.6 \mu\text{m} \times 1.6 \text{ nm}$). Therefore, the scattering force that is applied to a nanosheet in a perpendicular orientation should be 1000 times larger than that applied to a nanosheet in a parallel orientation. When the shape anisotropy, and thus the anisotropy of the scattering force that is applied to an object, is significant, such as nanowires^{24,25} and nanotubes,²⁶ it has been reported that the anisotropic particles are aligned parallel to the propagation direction of the incident laser beam to minimize the applied scattering force. The large anisotropy of the scattering force that is applied to the nanosheet should also result in a parallel orientation.

The domain that is formed at the focal point is ascribed to a scattering force and polarization direction of the electric field of incident laser beam. In this domain, nanosheets were aligned with their long axis parallel to the polarization direction of the laser beam. This alignment is rationalized by a previous study of electric alignment of niobate nanosheet liquid crystals.^{20,22} The trapped and electrically aligned nanosheets form a core around which nanosheets are assembled to produce the domain. However, the size is restricted to $\sim 15 \mu\text{m}$.

The domain at the periphery of the focal point is ascribed only to the scattering force. In this domain, a tree-ring-like nanosheet alignment that is independent of the laser polarization was observed. This result indicates that the orientational change is not caused by a gradient force. Based on a cylindrical alignment of nanosheets, the origin of this orientational change should be a scattering force that is applied to objects, and which corresponds to a Gaussian distribution of the radiation intensity of the irradiated laser beam.

Figure 6 shows a schematic representation of the orientational change. Before laser irradiation, the nanosheets are perpendicular to the propagation direction of the laser beam, but they are not strictly oriented (Figure 6a). With laser-beam irradiation, the nanosheets at the highest irradiance region are trapped rapidly to form a domain with a direction that

is dependent on the polarization direction of the laser beam (Figure 6b, the domain at the focal point is indicated by brown nanosheets). At the same time, nanosheets in a region where the scattering force is sufficient for a laser-induced orientational change (near to the focal point, indicated as a yellow background area in Figure 6) also start the orientational change, which proceeds gradually. Nanosheets, even at the outside of the beam path, are aligned because of the liquid crystallinity of the sample. Nanosheets near the aligned ones are drawn and aligned with nanosheet–nanosheet interactions. This process increases the population of aligned nanosheets in a cylindrical region around the beam path to form the peripheral domain (Figures 6c and 6d). Finally, nanosheets around the beam path are aligned sufficiently to provide a well-grown peripheral domain (Figure 6e). At this stage, the domain at the focal point with nanosheets that is oriented along the polarization direction is surrounded by nanosheets that are oriented into tree rings (cross-sectional image; Figure 6f). This model is consistent with textural changes that are observed by the polarized and bright-field microscope images. In addition, this model is also consistent with the power dependence of the texture size. When a laser beam of 100 mW was used, namely, the scattering force was enhanced, the diameter of the circular textured area grew to 200 μm (Supporting Information, Figure S4).

The contribution of thermal flow can be ruled out. The 20-mW laser-power irradiation was smaller by an order of magnitude than that used in conventional optical manipulation

studies in which thermal flow occurred. In addition, the sample consists of nanosheets and water does not absorb light at 532 nm. Movies in S1 and S2 indicate a wider sample area of $222\ \mu\text{m} \times 222\ \mu\text{m}$, which shows that the orientational change occurred only in a limited region of $110\ \mu\text{m}$ that is centered at the focal point, but the flow of nanosheets suggests that the occurrence of thermal flow was not observed.

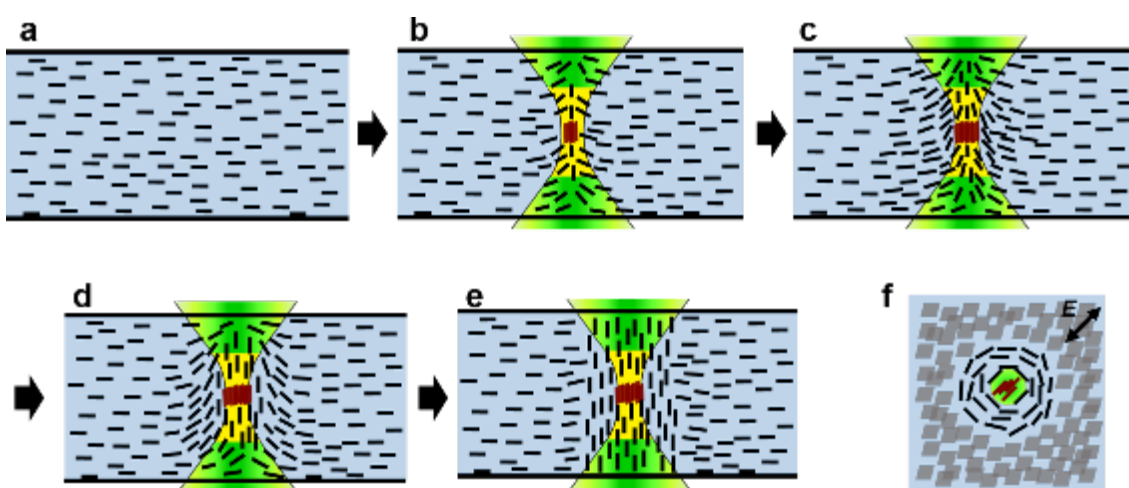


Figure 6. Schematic representation of orientational change of niobate nanosheets by laser radiation pressure (a–f). Cross-sectional image of Figure 6e in the focal plane. Nanosheets trapped at the focal point are indicated in brown. Green and yellow regions denote a beam path and an area with a high irradiance, respectively.

CONCLUSIONS

We have manipulated nanosheets in a colloidal dispersion to generate local but giant hierarchical structures. This structure consists of two domains. One is related mainly to an optical electric field and the other is attributed mainly to the scattering force of the incident laser beam. For the former domain, nanosheets at the focal point are oriented parallel to the polarization direction of the incident laser beam. This is common to isotropic and liquid-crystalline nanosheet colloids. However, the latter giant domain

evolves only in the liquid-crystalline nanosheet colloid. The hierarchical structure is achieved by a scattering force of the incident laser beam, which aligns the micron-sized nanosheets that cooperate with each other in a liquid-crystalline state into a rather large scale. Hence, laser radiation pressure can be used to construct hierarchical colloidal structures of subnanometer to submicron scales with the aid of interparticle interactions in the colloids. The optical manipulation of colloidal liquid-crystalline nanosheets established in this study provides a powerful method to achieve a variety of on-demand orientations of nanosheets. These results expand the application of nanosheets to their use in optical switches, light modulators, and so forth.

METHODS

Sample Preparation. Single-crystalline $\text{K}_4\text{Nb}_6\text{O}_{17}$ was prepared by a flux method; a mixture of K_2CO_3 (Wako Pure Chemical Industries, Ltd., Japan) and Nb_2O_5 (Soekawa Chemicals Co., Ltd., Japan) was heated at 1150°C and cooled gradually^{20,21}. $\text{K}_4\text{Nb}_6\text{O}_{17}\cdot 3\text{H}_2\text{O}$ (1 g) was treated with a 0.2 mol dm^{-3} aqueous solution of propylammonium chloride (Tokyo Chemical Industry Co., Ltd., Japan) at 120°C for one week to exchange the interlayer potassium ions for propylammonium ions. The reaction product was centrifuged at 11000 rpm, washed, and dialyzed with water to yield a stock sample of niobate nanosheet colloid. The niobate nanosheet colloid sample was diluted with water to 0.05 and 5 gL^{-1} of the niobate concentration (indicated as the mass of $[\text{Nb}_6\text{O}_{17}]^{4-}$). The lateral lengths of the nanosheets that were obtained from TEM observations had a size distribution that obeyed a log-normal distribution to yield an average size of $1.6 \mu\text{m}$. The colloids that were prepared at concentrations of 0.05 gL^{-1} and 5 gL^{-1} exhibited an isotropic and biphasic mixture of isotropic and liquid-crystalline

phases at room temperature, respectively.

Optical microscope observation. The sample was injected into a 100- μm thick thin-layer glass cell. The cell was set on the stage of an inverted microscope (IX70, Olympus). A linearly polarized CW Gaussian laser beam that emits at 532 nm (Millennia Pro, Spectra Physics) was focused at the center of the cell (50 μm from the cell surface) using a water-immersion objective lens (UPlanSApo, Olympus, 60 \times , N.A. = 1.20) at room temperature. The laser power was set to 20 mW after the objective lens unless otherwise noted. The beam diameter was adjusted to the pupil diameter of the objective lens by using a beam expander. The resulting beam waist at the focal point was calculated to be 0.3 μm . The polarization direction of the laser beam was controlled by rotating a half-wave plate. For polarized optical microscope observations with a linearly polarized laser beam irradiation, the sample was illuminated by a halogen lamp, and the image was monitored with a digital CMOS camera (ORCA-Flash 4.0 V3, Hamamatsu Photonics). A pair of crossed polarizers (polarizer and analyzer) were inserted out of the beam pass of the laser beam. Bright-field optical microscope images were observed using the same optical setup without a polarizer and an analyzer. We confirmed that the laser beam was blocked completely by a dichroic mirror and a band pass filter that was inserted before the camera. Spatial resolutions in our setup were 330 nm. These values were almost the same size as the diffraction limits.

ASSOCIATED CONTENT

Supporting Information

Contrast-adjusted polarized optical microscope images of Figures 2c and 2d (Figure S1); bright-field optical microscope images magnified at focal point of Figures 3b and 3e (Figure S2); polarized optical microscope image of an isotropic niobate nanosheet colloid

(Figure S3); polarized optical microscope image of a liquid-crystalline niobate nanosheet colloid when a laser beam of 100 mW was irradiated (Figure S4); video image of a liquid-crystalline niobate nanosheet colloid observed with a polarized optical microscope during laser irradiation (Movie S1); video image of a liquid-crystalline niobate nanosheet colloid observed with a bright-field optical microscope during laser irradiation (Movie S2); video image of an isotropic niobate nanosheet colloid observed with a bright-field optical microscope during laser irradiation (Movie S3).

AUTHOR INFORMATION

Corresponding Author

*E-mail: nakato@che.kyutech.ac.jp.

*E-mail: j_kawa@yamaguchi-u.ac.jp.

Notes

The authors declare no competing financial interest.

ACKNOWLEDGMENTS

This work was supported by JSPS KAKENHI Grant Numbers 15J07557 (M.T.), 15H03878 (T.N.), 17H05466 (Y.S.), and 15K13676 (J.K.), and by the Opto-Energy Research Center in Yamaguchi University. M.T. was supported financially by a JSPS Research Fellowship for Young Scientists. We thank Laura Kuhar, PhD, from Edanz Group (www.edanzediting.com/ac) for editing a draft of this manuscript.

REFERENCES

(1) Demirörs, A. F.; Beltramo, P. J.; Vutukuri, H. R. Colloidal switches by electric and

- magnetic fields. *ACS Appl. Mater. Interfaces* **2017**, *9*, 17238-17244.
- (2) Lisjak, D.; Jenuš, P.; Mertelj, A. Influence of the morphology of ferrite nanoparticles on the directed assembly into magnetically anisotropic hierarchical structures. *Langmuir* **2014**, *30*, 6588-6595.
- (3) Lee, W.; Kim, S.; Kim, S.; Kim, J. H.; Lee, H. Hierarchical opal grating films prepared by slide coating of colloidal dispersions in binary liquid media. *J. Colloid Interface Sci.* **2015**, *440*, 229-235.
- (4) Rodrigo, P. J.; Daria, V. R.; Glückstad, J. Four-dimensional optical manipulation of colloidal particles. *Appl. Phys. Lett.* **2005**, *86*, 074103.
- (5) Shoji, T.; Shibata, M.; Kitamura, N.; Nagasawa, F.; Takase, M.; Murakoshi, K.; Nobuhiro, A.; Mizumoto, Y.; Ishihara, H.; Tsuboi, Y. Reversible photoinduced formation and manipulation of a two-dimensional closely packed assembly of polystyrene nanospheres on a metallic nanostructure. *J. Phys. Chem. C* **2013**, *117*, 2500-2506.
- (6) Toyoda, K.; Takahashi, F.; Takizawa, S.; Tokizane, Y.; Miyamoto, K.; Morita, R.; Omatsu, T. Transfer of light helicity to nanostructures. *Phys. Rev. Lett.* **2013**, *110*, 143603.
- (7) Wright, W. H.; Sonek, G. J.; Berns, M. W. Parametric study of the forces on microspheres held by optical tweezers. *Appl. Opt.* **1994**, *33*, 1735-1748.
- (8) Ashkin, A.; Dziedzic, J. M.; Bjorkholm, J. E.; Chu, S. Observation of a single-beam gradient force optical trap for dielectric particles. *Opt. Lett.* **1986**, *11*, 288-290.
- (9) Shoji, T.; Kitamura, N.; Tsuboi, Y. Resonant excitation effect on optical trapping of myoglobin: the important role of a heme cofactor. *J. Phys. Chem. C* **2013**, *117*, 10691-10697.
- (10) Misawa, H.; Koshioka, M.; Sasaki, K.; Kitamura, N.; Masuhara, H. Three-dimensional optical trapping and laser ablation of a single polymer latex particle in water.

J. Appl. Phys. **1991**, *70*, 3829.

(11) Inaba, K.; Imaizumi, K.; Katayama, K.; Ichimiya, M.; Ashida, M.; Iida, T.; Ishihara, H.; Itoh, T. Optical manipulation of CuCl nanoparticles under an excitonic resonance condition in superfluid helium. *Phys. Stat. Sol. (b)* **2006**, *243*, 3829-3833.

(12) Olof, S. N.; Grieve, J. A.; Phillips, D. B.; Rosenkranz, H.; Yallop, M. L.; Miles, M. J.; Patil, A. J.; Mann, S.; Carberry, D. M. Measuring nanoscale forces with living probes. *Nano Lett.* **2012**, *12*, 6018-6023.

(13) Wu, M. Y.; Ling, D. X.; Ling, L.; Li, W.; Li, Y. Q. Stable optical trapping and sensitive characterization of nanostructures using standing-wave Raman tweezers. *Sci. Rep.* **2017**, *7*, 42930.

(14) Usman, A.; Uwada, T.; Masuhara, H. Optical reorientation and trapping of nematic liquid crystals leading to the formation of micrometer-sized domain. *J. Phys. Chem. C* **2011**, *115*, 11906-11913.

(15) Wang, S. F.; Yuyama, K.; Sugiyama, T.; Masuhara, H. Reflection microspectroscopic study of laser assembling of polystyrene nanoparticles at air/solution interface. *J. Phys. Chem. C* **2016**, *120*, 15578-15585.

(16) Wang, S. F.; Kudo, T.; Yuyama, K.; Sugiyama, T.; Masuhara, H. Optically evolved assembly formation in laser trapping of polystyrene nanoparticles at solution surface. *Langmuir* **2016**, *32*, 12488-12496.

(17) Kudo, T.; Wang, S. F.; Yuyama, K.; Masuhara, H. Optical trapping-formed colloidal assembly with horns extended to the outside of a focus through light propagation. *Nano Lett.* **2016**, *16*, 3058-3062.

(18) Nakato, T.; Miyamoto, N. Liquid crystalline behavior and related properties of colloidal systems of inorganic oxide nanosheets. *Materials* **2009**, *2*, 1734-1761.

- (19) Yamaguchi, D.; Miyamoto, N.; Fujita, T.; Nakato, T.; Koizumi, S.; Ohta, N.; Yagi, N.; Hashimoto, T. Aspect-ratio-dependent phase transitions and concentration fluctuations in a aqueous colloidal dispersions of charged platelike particles. *Phys. Rev. E* **2012**, *85*, 011403.
- (20) Nakato, T.; Nono, Y.; Mouri, E.; Nakata, M. Panoscopic organization of anisotropic colloidal structures from photofunctional inorganic nanosheet liquid crystals. *Phys. Chem. Chem. Phys.* **2014**, *16*, 955-962.
- (21) Miyamoto, N.; Nakato, T. Liquid crystalline nanosheet colloids with controlled particle size obtained by exfoliating single crystal of layered niobate $K_4Nb_6O_{17}$. *J. Phys. Chem. B* **2004**, *108*, 6152-6159.
- (22) Nakato, T.; Nakamura, K.; Shimada, Y.; Shido, Y.; Houryu, T.; Iimura, Y.; Miyata, H. Electrooptic response of colloidal liquid crystals of inorganic oxide nanosheets prepared by exfoliation of a layered niobate. *J. Phys. Chem. C* **2011**, *115*, 8934-8939.
- (23) Nakato, T.; Nono, Y.; Mouri, E. Textural diversity of hierarchical macroscopic structures of colloidal liquid crystalline nanosheets organized under electric fields. *Colloid Surf., A* **2017**, *522*, 373-381.
- (24) Reece, P. J.; Paiman, S.; Abdul-Nabi, O.; Gao, Q.; Gal, M.; Tan, H. H.; Jagadish, C. Combined optical trapping and microphotoluminescence of single InP nanowires. *Appl. Phys. Lett.* **2009**, *95*, 101109.
- (25) Lee, S. W.; Jo, G.; Lee, T.; Lee, Y. G. Controlled assembly of In_2O_3 nanowires on electronic circuits using scanning optical tweezers. *Opt. Exp.* **2009**, *20*, 17491-17501.
- (26) Maragò, O. M.; Jones, P. H.; Bonaccorso, F.; Scardaci, V.; Gucciardi, P. G.; Rozhin, A. G.; Ferrari, A. C. Femtonewton force sensing with optically trapped nanotubes. *Nano Lett.* **2008**, *10*, 3211-3216.

For Table of Contents Use Only

Radiation-Pressure-Induced Hierarchical Structure of Liquid-Crystalline Inorganic Nanosheets

Makoto Tominaga, Takashi Nagashita, Takuya Kumamoto, Yuki Higashi, Toshiaki Iwai, Teruyuki Nakato, Yasutaka Suzuki, Jun Kawamata

A local and huge hierarchical structure of liquid-crystalline nanosheets was constructed by combining a laser radiation pressure and the liquid crystallinity of a nanosheet.

